

# An antenna switching based NOMA scheme for IEEE 802.15.4 concurrent transmission

Xianjun Jiao, Muhammad Aslam, Wei Liu, Ingrid Moerman  
IDLab, Ghent University - imec, Gent, Belgium  
xianjun.jiao@ugent.be

**Abstract**—This paper introduces a Non-Orthogonal Multiple Access (NOMA) scheme to support concurrent transmission of multiple IEEE 802.15.4 packets. Unlike collision avoidance Multiple Access Control (MAC), concurrent transmission supports Concurrent-MAC (C-MAC) where packet collision is allowed. The communication latency can be reduced by C-MAC because a user can transmit immediately without waiting for the completion of other users' transmission. The big challenge of concurrent transmission is that error free demodulation of multiple collided packets hardly can be achieved due to severe Multiple Access Interference (MAI). To improve the demodulation performance with MAI presented, we introduce an architecture with multiple switching antennas sharing a single analog transceiver to capture spatial character of different users. Successive Interference Cancellation (SIC) algorithm is designed to separate collided packets by utilizing the spatial character. Simulation shows that at least five users can transmit concurrently to the SIC receiver equipped with eight antennas without sacrificing Packet Error Rate.

**Keywords**—IEEE 802.15.4, MIMO, Switching Antenna, NOMA, SIC, CDMA, C-MAC

## I. INTRODUCTION

Internet of Things (IoT) technology has been used widely in industrial communication scenario. In some critical industrial applications, such as emergency break/stop, latency is a key performance aspect. When there are many users/nodes in the industrial deployment, it is difficult to achieve low latency communication because of the nature of spectrum sharing. Multiple users have to follow some Media Access Control (MAC) mechanism, such as Carrier Sensing Multiple Access Collision Avoidance (CSMA/CA) or Time Division Multiple Access (TDMA), to avoid collision in the same frequency channel. It means that users need to transmit one after another. When the channel is very busy, users will suffer a lot on data rate and latency. The low data rate is because all users sharing the single channel capacity. The high latency is because transmission has to wait for long time before channel becomes idle.

In [1-2], co-channel concurrent transmission was introduced. It is based on a phenomenon observed in an IEEE 802.15.4 experiment: even two packets are colliding with each other, there is still a big chance to decode both packets correctly if their relative power is the same/similar. If power difference is too big, only the strong packet can be decoded because the weak packet suffers too much interference caused by the strong packet. By living with collision, the Concurrent Media Access Control (C-MAC) was proposed to increase the system capacity and

lower the latency, because multiple users are allowed to transmit at the same time.

The concept of multi-user concurrent transmission can be traced back to Code Division Multiple Access (CDMA) system [3]. Successive Interference Cancellation (SIC) architecture is a promising Multi-User Detector (MUD) scheme to detect multi-user Non-strict-Orthogonal CDMA signal. As a successor of the MUD concept, Non Orthogonal Multiple Access (NOMA) was proposed as part of 5G technology [4-5]. In the typical NOMA design, user power and beamforming weights need to be scheduled/allocated carefully to ensure that SIC works in the best situation. Forward Error Correction (FEC) also plays an important role for successful demodulation under severe interference during SIC iterations.

Spatial Division Multiple Access (SDMA) or Multiple Input Multiple Output (MIMO) is another way to achieve concurrent transmission, and has become the key technology in Wi-Fi, 4G and 5G systems [6-8]. However, typical MIMO scheme requires the same number of RF transceivers as the number of antennas. In massive MIMO, the massive RF transceivers lead to significant cost, power consumption and weight, which are very challenging for implementation.

In this paper, we propose a co-channel concurrent transmission scheme based on antenna switching. In our design, multiple antennas share a single RF transceiver, and capture spatial character of transmission from different users. Together with SIC operation, multi-user signals can be demodulated successfully utilizing spatial character of different users. IEEE 802.15.4 O-QPSK physical layer is taken as an example. The scheme can also be applied to other system, where multiple users sharing the same set of spreading sequence, such as the Physical Random Access Channel (PRACH) in 4G/5G and GPS system. The remaining part of this paper is organized as following: section II introduces traditional IEEE 802.15.4 transceiver and the interference model of concurrent transmission; section III proposes the NOMA scheme based on antenna switching and SIC procedure; section IV shows the Packet Error Rate (PER) simulation result of multi-user concurrent transmission under different array size; section V discusses synchronization, power differences and uplink/downlink reciprocal operation; section VI compares our work and the related work; section VII concludes the paper.

## II. IEEE 802.15.4 TRANSCIVER AND INTERFERENCE MODEL

### A. Transmitter and receiver

Figure 1 shows the processing steps of the transmitter defined in IEEE 802.15.4-2015 standard [9]. In the O-QPSK 250k bit/s PHY definition (section 12.2.4 of [9]), every 4 bits,

also known as a symbol, are mapped to a length 32 chip sequence as shown in Table I (Table 12-1 of [9]).

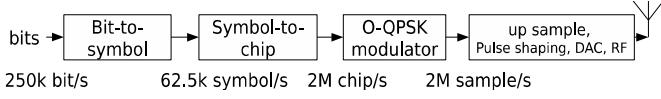


Fig. 1. IEEE 802.15.4 O-QPSK 250k bit/s transmitter

TABLE I. IEEE 802.15.4 SYMBOL-TO-CHIP MAPPING FOR THE 2450 MHz AND 2380 MHz BAND

Data symbol	Chip values ( $c_0 \ c_1 \dots \ c_{30} \ c_{31}$ )
0	11011001110000110101001000101110
1	11101101100111000011010100100010
2	00101110110110011100001101010010
3	00100010111011011001110000110101
4	01010010001011101101100111000011
5	00110101001000101110110110011100
6	11000011010100100010111011011001
7	10011100001101010010001011101101
...	...
15	11001001011000000111011110111000

Notice that the first 8 chip sequences are cyclic shifted version of the chip sequence for data symbol 0. The last 8 chip sequences are cyclic shifted version of the chip sequence for data symbol 8. This leads to severe interference, which will be further elaborated in later sections.

The receiver performs the inverse processing of transmitter. The core step is determining which chip sequence has been transmitted by the transmitter. To detect the sequence index, the following correlation test method can be used.

$$i = \underset{i=0 \dots 15}{\operatorname{argmax}} \{ \mathbf{s}_i^H \times \mathbf{r} \} \quad (1)$$

Where  $\mathbf{s}_i$  is  $32 \times 1$  vector representing the  $i$ th chip sequence defined in the standard (O-QPSK modulated version);  $\mathbf{r}$  is  $32 \times 1$  vector representing synchronized incoming I/Q sample. Superscript  $\mathbf{H}$  means conjugate transpose. The formula correlates input signal with 16 predefined chip sequences, and the one that generates the biggest correlation result implies the most possible transmitted sequence.

### B. Interference model

The correlation test method (1) will be unreliable if another time shifted chip sequence is transmitted concurrently by another user. For example, in Figure 2 an interfering signal has relative time difference around  $8\mu\text{s}$  (4 chips) in parallel to the target signal, and both users transmit chip sequence 5. In this case, not only local chip sequence 5 but also local chip sequence 4 will generate strong correlation value. Because from the beginning time of the target sequence, the interferer signal segment becomes part of chip sequence 4, although the interferer is also transmitting chip sequence 5.

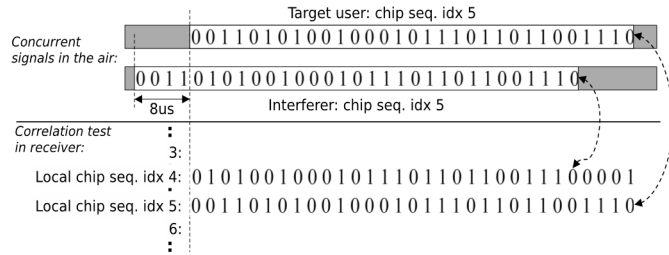


Fig. 2. IEEE 802.15.4 interference and correlation test model.

In theory, sequence 4's correlation value is weaker than sequence 5's because the interferer only gives a partial sequence, therefore the target user's sequence 5 can still be identified correctly. In practice, the mistaken probability of correlation test is high, because the correlation value of chip sequence 4 is also big.

### III. ANTENNA SWITCHING BASED NOMA SCHEME

According to the analysis of the previous section, multi-user signals are Non-Orthogonal because there is only one set of chip sequence in the IEEE 802.15.4 standard and all users use the same sequence set for modulation instead of Multiple Accessing (MA). This is different from the traditional CDMA system, where individual users are assigned with different sequences for MA. Because of this, separation of different user signals becomes difficult for IEEE 802.15.4 concurrent transmission. Considering that different users are usually located in different locations in real deployment, an antenna array can be used to capture this spatial character. The different spatial array responses will render the same set of chip sequence to different sets for different users at different locations. Figure 3 shows how to achieve this via switching antennas and a single RF receiver. In our design, antenna switching rate is the same as chip rate. In this example, three users are transmitting concurrently and multi-user receiver is equipped with 4 switching antennas. There are three separated baseband processing branches to extract bits of three users.

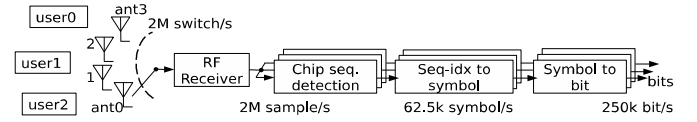


Fig. 3. Antenna switching based multi-user receiver

#### A. Chip sequence detection involving spatial character

The signal model at chip sequence detection of the proposed multi-user receiver is depicted in Figure 4.

User idx	Signal Model																																
0	$c_{0,0} \cdot h_{0,0}$	$c_{0,1} \cdot h_{0,1}$	$c_{0,2} \cdot h_{0,2}$	$c_{0,3} \cdot h_{0,3}$	$c_{0,4} \cdot h_{0,0}$	...	$c_{0,31} \cdot h_{0,3}$	$c_{0,0} \cdot h_{0,0}$	$c_{0,1} \cdot h_{0,1}$	...																							
1	$c_{1,28} \cdot h_{1,0}$	$c_{1,29} \cdot h_{1,1}$	$c_{1,30} \cdot h_{1,2}$	$c_{1,31} \cdot h_{1,3}$	$c_{1,0} \cdot h_{1,0}$	...	$c_{1,27} \cdot h_{1,3}$	$c_{1,28} \cdot h_{1,0}$	$c_{1,29} \cdot h_{1,1}$	...																							
2	$c_{2,31} \cdot h_{2,0}$	$c_{2,0} \cdot h_{2,1}$	$c_{2,1} \cdot h_{2,2}$	$c_{2,2} \cdot h_{2,3}$	$c_{2,3} \cdot h_{2,0}$	...	$c_{2,30} \cdot h_{2,3}$	$c_{2,31} \cdot h_{2,0}$	$c_{2,0} \cdot h_{2,1}$	...																							
	0	1	2	3	4		31	32	33	samp idx																							
	0	1	2	3	0		3	0	1	Ant idx																							

Fig. 4. Signal model of multi-user concurrent transmission

Y axis indexes user. X axis indexes the received I/Q sample and the corresponding antenna (remember that antenna switching rate is the same as baseband chip rate). In general, multi-user transmissions are asynchronous, and different user signals have different time shifts at receiver. Although we draw signal of different users separately with different user indexes in Figure 4, actually they are superposed at the point of RF receiver in Figure 3. The task of chip sequence detection is identifying different chip sequences transmitted by different users. In Figure 4, the series of white block represent a complete chip sequence of a user, and gray blocks are chips from adjacent symbol of the same user.  $cn_j$  is the I/Q sample of the  $n$ th user's  $j$ th chip, where  $n=\{0,1,2\}$  and  $j=\{0,1,\dots,31\}$ .  $hn_k$  is complex channel gain between the  $n$ th user and the  $k$ th antenna, where  $n=\{0,1,2\}$ ,  $k=\{0,1,2,3\}$ . With this model, the chip sequence detection for user  $n$  will be:

$$i = \underset{i=0 \dots 15}{\operatorname{argmax}} \{ \mathbf{s}_{n,i}^H \times \mathbf{r}_n \} \quad (2)$$

Where  $\mathbf{r}_n$  is  $32 \times 1$  vector:

$$\mathbf{r}_n = \begin{bmatrix} r_{q(n)+0} \\ r_{q(n)+1} \\ \vdots \\ r_{q(n)+31} \end{bmatrix} \quad (3)$$

representing the corresponding segment of incoming I/Q sequence of user  $n$ .  $q(n)$  is the starting I/Q sample index of a chip sequence for user  $n$ . In the example depicted in Figure 4, for user 0,  $q(0)=0$ , which means the I/Q sample indexes for a symbol are 0~31; for user 1,  $q(1)=4$ , which means the I/Q sample indexes for a symbol are 4~35; for user 2,  $q(2)=1$  which means I/Q sample indexes for a symbol are 1~32. So, the segment  $\mathbf{r}_n$  contains a complete chip sequence from the  $n$ th user and interference from other users.  $\mathbf{s}_{n,i}$  is not the standard chip sequence  $\mathbf{s}_i$  in (1) anymore, instead  $\mathbf{s}_{n,i}$  is the antenna switching scrambled version of the original chip sequence:

$$\mathbf{s}_{n,i} = \begin{bmatrix} s_{i,0} \cdot h_{n,[q(n)+0] \bmod 4} \\ s_{i,1} \cdot h_{n,[q(n)+1] \bmod 4} \\ \vdots \\ s_{i,31} \cdot h_{n,[q(n)+31] \bmod 4} \end{bmatrix} \quad (4)$$

Where  $h_{n,k}$  is complex channel gain between the  $n$ th user and the  $k$ th antenna;  $k = [q(n) + \{0 \dots 31\}] \bmod 4$  and  $\bmod$  means modulo operation;  $h_{n,k}$  is the unique spatial character captured by switching antenna. This spatial scrambling operation generates different chip sequence sets for different users, thus it reduces the multi-user interference which is very strong in a single antenna receiver as analyzed in section II B.

### B. Successive Interference Cancellation (SIC)

In the SIC operation of NOMA receiver, interference cancellation of the strong users improves the detection performance of the weak users. Figure 5 shows the proposed SIC procedure for IEEE 802.15.4 multi-user receiver.

In an SIC iteration, if some decoded packets pass CRC check, the corresponding signals will be reconstructed and subtracted. Even if there isn't any decoded packet passing CRC check, we propose reconstructing signal based on bits decoded from the signal that has strong correlation value, because that implies a high chance to have more correct bits. This is called non-ideal reconstruction. If this happens in an iteration, the subtracted signal will be recovered in the next iteration by the inter-iteration store-restore operation (*restore\_flag* in Figure 5), so that more decoding attempts can be performed on the original signal. In this way, the chance of successful decoding is improved.

### C. Dual chip sequence detection

To increase the chip sequence detection reliability under strong interference, two successive chip sequences can be detected together. The received I/Q sequence (length 64 instead of 32) is correlated with 256 (instead of 16) equivalent local chip sequences to find out which pair of chip sequences is transmitted. In this way, the correlation length is doubled, thus higher processing gain is achieved. The new 256 equivalent chip sequences are generated by cascading two original chip sequences:

$$\mathbf{b}_k = \begin{bmatrix} \mathbf{s}_i \\ \mathbf{s}_j \end{bmatrix}, k = 16 \cdot i + j \quad (5)$$

Where  $\mathbf{s}_x, x \in \{0, \dots, 15\}$  represents the  $x$ th original chip sequence.  $\mathbf{b}_k, k \in \{0, 255\}$  is the new equivalent chip sequence set.

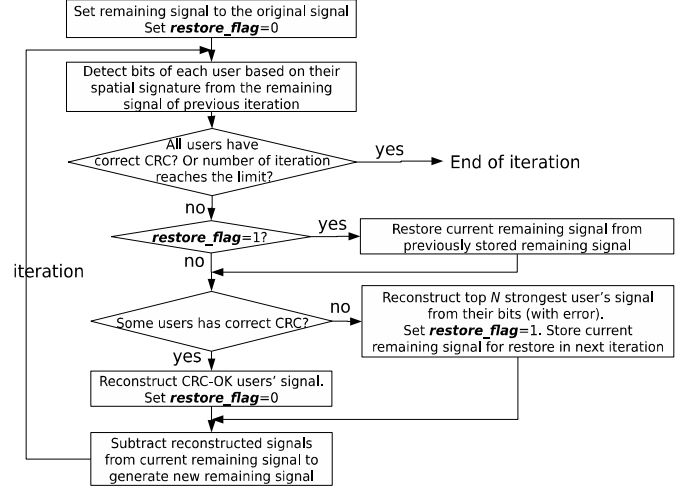


Fig. 5. SIC procedure for IEEE 802.15.4 multi-user receiver

## IV. SIMULATION RESULTS

To evaluate the antenna switching based NOMA SIC algorithm, numerical simulation is carried out involving a model of uniform circular array composed by 8 antennas. The corresponding simulation topology is shown in Figure 6. Multiple users are located at specific directions with equal angle spacing. Line of Sight (LoS) propagation model and far-field plane wave model are used to calculate the multiple complex channel gains. The arrival time of signals from different users are distributed randomly in the time interval of 16 $\mu$ s (time duration of chip sequence) to model the asynchronous behavior of concurrent users. For the best performance, parameter  $N$  ("Reconstruct top  $N$  strongest ..." in Figure 5) is set to 2 in our case. The maximum number of iteration is set to the number of concurrent users. Each simulation result is the averaging of multiple simulation results on direction angle 0, 9, 18, ..., 45 degrees. Thanks to the symmetric array, 0~360 degree ergodic tests are not necessary.

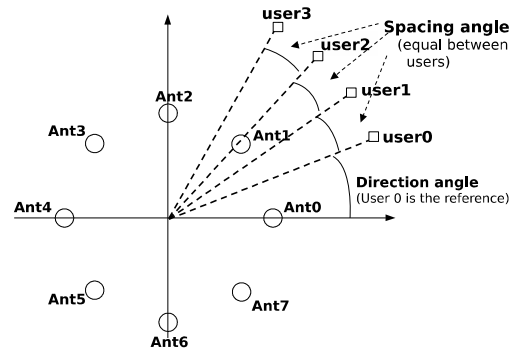


Fig. 6. Simulation setup of antenna array and multiple users

Figure 7 give the simulated PER results under different array diameter, number of user, spacing angle, detection method and power difference.

In the PER figure, “1 seq” and “2 seq” refer to single chip sequence detection and dual chip sequence detection accordingly; “XXdB power diff” means that received multi-user signal strengths (relative level) is distributed randomly between 0dB to XXdB. The larger dB value means the bigger chance to have a stronger user for the successful decoding in the 1st SIC iteration. Zero dB means the worst case where all users generate the same received power at multi-user receiver. This is confirmed in the simulation results: The bigger user power difference supports more concurrent users. Five users can transmit concurrently achieving 1% PER under the worst case of 0dB power difference. When array diameter is 16cm, spacing between user needs to be not less than 20 degrees. With a 32cm diameter array, spacing angel can be as small as 10 degrees.

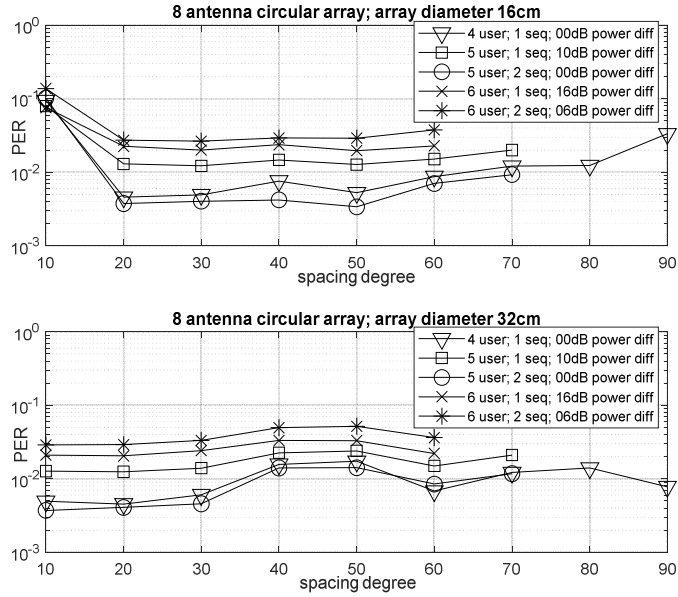


Fig. 7. Averaged simulation results of 16cm and 32cm diameter array

## V. FURTHER DISCUSSION

### A. Synchronization and channel estimation

Previous analysis and simulation assume that receiver knows different user signals’ arrival time and channel complex gains. In practice, this information can be estimated based on pre-known unique sequence sent by the user. The unique sequence could be the identity of the user, such as MAC address, serial number or temporary assigned identity. After initial handshaking/discovery/registration procedure (non-concurrent transmission), multi-user receiver can know the unique sequence of different users to assist future synchronization during concurrent transmission.

To ease the synchronization and channel estimation during the concurrent transmission phase, another parallel receiver chain and dedicated antenna can be added. The unique sequence of each user can be searched continuously via the dedicated antenna. Meanwhile we keep buffering I/Q samples from the switching antenna array. After identifying the arrival time of specific user’s unique sequence, I/Q samples of the same sequence has also been received via switching antenna and stored in the buffer. These I/Q samples can be used to estimate channel between the user and each switching antenna. This

architecture is shown in Figure 8. If extra time consumption is acceptable, the parallel searching task performed by the parallel receiver can be serialized with NOMA detection. Then the parallel receiver is not needed any more. Instead, the switching branch can work in non-switching mode firstly, then switching mode.

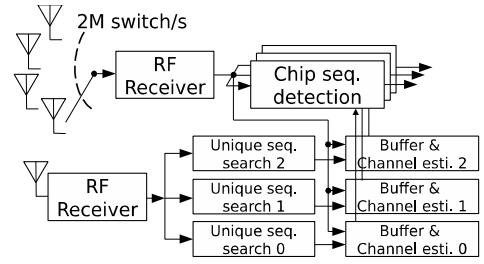


Fig. 8. Parallel processing chain assisted synchronization

Please be noticed that all above processing is based on 2M sample/s which is the chip rate of 802.15.4 standard (O-QPSK 250k bit/s mode). In practice, the front-end Analog-to-Digital Converter (ADC) uses a higher sampling rate, such as 8M samples/s and during synchronization (unique sequence search) the best sample (1 out of 4 for example) will be extracted. This decimation processing will generate I/Q sample at 2M sample/s from the 8M sample/s of ADC. This decimation step is now shown in this paper.

### B. Power differences

In traditional NOMA design, users with very different received signal strengths can be scheduled for concurrent transmission, because the successful rate of the 1<sup>st</sup> iteration can be high by decoding the strongest user firstly. But this scheduling needs extra signaling overhead. In addition, very different received signal strengths requires multi-user RF receiver to support high dynamic range, and Analog-to-Digital Converter (ADC) to be high resolution. This kind of high quality hardware could lead to significant increment in cost and power consumption.

The purpose of power control in IoT system is having the minimum required received power (right above the sensitivity level) at the receiver, so that user transmitting power can be saved and potential interference can be decreased. This equal received power at receiver leads to the worst case for SIC, as explained in the simulation section, because it is difficult to find a user with high Signal to Interference and Noise Ratio (SINR) for the 1<sup>st</sup> iteration. Our design works well under this worst condition (“0dB power diff” in simulation), thus complicated user scheduling is not necessary in our scheme.

### C. Downlink operation

Previous description focuses on the case where multiple users transmit to one receiver concurrently. The concurrent transmission can also be implemented in downlink: from one transmitter to multiple users. Thanks to the half-duplex mode, the channel estimation result in uplink is also valid in downlink after calibration procedure. There are two options to use the channel information in downlink operation. The transmitter can pre-compensate channel gain for each user’s receiver before transmission. Or the receiver uses the channel character, when performing chip sequence detection just like multiple parallel

chip sequence detections in multi-user receiver. In downlink operation, SIC algorithm runs in each user's receiver. To get user's own bits in its receiver, other users' bits might need to be decoded during SIC iteration. This privacy/security issue is interesting but not in this paper's scope.

## VI. COMPARISON WITH RELATED WORK

Typical MIMO solutions in Wi-Fi, 4G and 5G [6-8] involve full-time spatial sampling by many parallel antennas and RF transceivers, which are costly and power hungry. By complicated scheduling, different physical layer bit rate can fit into the capacity of different spatial streams. In [10-11], MIMO and NOMA scheme were researched for IoT system like IEEE 802.15.4, and some benefits are shown. However, in those works, each antenna has dedicated RF transceiver. On the contrary, low power IoT system has fixed physical layer bit rate and is sensitive to cost/power-consumption. Our design uses single RF transceiver switching between passive antennas, and more digital processing to handle concurrent transmission. This choice makes sense because RF/analog IC never scale as efficient as digital IC (Moore's law), and passive antennas only add minor cost. So it will be a cost and power effective solution. Also thanks to more and more powerful digital processing capability, SIC won't involve too much latency to the low data rate IoT system.

In traditional NOMA design [4-5], users need to be selected carefully to help the SIC operation as explained before. To achieve this, keep-alive close-loop signaling/control is used in typical NOMA system. While our scheme doesn't need user power scheduling, and still works well in the worst case. This signaling less design could ease the application of our scheme to light weight IoT system, where the mode of "occasionally transmit then long sleep" is preferred.

Reference [12] uses multiple antennas in a switching way to increase the bit rate of single user. When transmitting,  $\log_2(N)$  bits drive a selector to choose one antenna from  $N$  antennas. To demodulate the extra bits, the receiver needs to identify the transmitting antenna according to the channel gain knowledge of different antennas. Both transmitter and receiver are not compliant with any IoT standard anymore. While our scheme targets multi-user concurrent transmission instead of rate boosting for a single user, and our approach doesn't need the IEEE 802.15.4 physical layer to be changed. Our multi-user receiver can work with legacy IEEE 802.15.4 compliant sensor node. It means that only the gateway of an already deployed IoT network needs to be upgraded to improve the network throughput and latency performance.

Reference [13-14] proposes the switching antenna based MIMO, but the switching speed is multiple times of baseband symbol rate: "the purpose of the switch is the capture of the signals of all the antennas for every symbol time interval of the modulated signal". That means bandwidth of RF chain needs to be several times larger than the baseband requirement, thus it aliases interference from several adjacent frequency channels. While in our scheme the antenna switching rate is the same as the baseband rate (chip rate 2M in IEEE 802.15.4 250k bit/s mode for example). So, RF transceiver works in normal bandwidth configuration as the traditional IEEE 802.15.4

transceiver, and the issue of multi-channel aliasing interference doesn't exist in our scheme.

## VII. CONCLUSION

A hardware efficient NOMA scheme is designed for concurrent transmission in low power IoT system, such as IEEE 802.15.4, to improve the throughput and latency performance of the network. In the design, a single RF transceiver together with switching antennas are used to capture the spatial character of different IoT users at different locations. The SIC algorithm is designed to separate multi-user signals utilizing their different spatial characteristics. Simulation shows that at least 5 users can transmit concurrently and be demodulated successfully at multi-user SIC receiver, equipped with a 16cm 8-antenna array. The scheme doesn't need sophisticated user power scheduling, which is generally required in conventional NOMA design, and can operate with legacy 802.15.4 node. So it is a suitable solution for light-weight signaling-free IoT systems, and also an ideal option to upgrade existing IoT systems.

## REFERENCES

- [1] M. Sha, G. Xing, G. Zhou, S. Liu, and X. Wang, "C-MAC: model-driven concurrent medium access control for wireless sensor networks," in Proc. INFOCOM, Rio de Janeiro, Brazil, Apr. 2009, pp. 1845-1853.
- [2] M. Wilhelm, V. Lenders, and J. B. Schmitt. An Analytical Model of Packet Collisions in IEEE 802.15.4 Wireless Networks. CoRR, abs/1309.4, 2013.
- [3] X. Wang and H. V. Poor, "Iterative (Turbo) soft interference cancellation and decoding for coded CDMA," IEEE Transactions on Communications, vol. 47, no. 7, pp. 1046-1061, Jul 1999.
- [4] Y. Saito, Y. Kishiyama, A. Benjebbour, T. Nakamura, A. Li, K. Higuchi, "Non-orthogonal multiple access (NOMA) for cellular future radio access", Proc. IEEE VTC, pp. 1-5, Jun. 2013.
- [5] M. S. Ali, E. Hossain, and D. Kim, "Non-orthogonal multiple access (NOMA) for downlink multiuser MIMO systems: User clustering, beamforming, and power allocation," IEEE Access, vol. 5, pp. 565-577, 2017.
- [6] Huacheng Zeng, Hongxiang Li, and Qiben Yan. 2018. Uplink MU-MIMO in Asynchronous Wireless LANs. In Proceedings of the Eighteenth ACM International Symposium on Mobile Ad Hoc Networking and Computing (Mobihoc '18). ACM, New York, NY, USA, 21-30.
- [7] A. F. Molisch et al., "Hybrid Beamforming for Massive MIMO: A Survey," in IEEE Communications Magazine, vol. 55, no. 9, pp. 134-141, Sept. 2017.
- [8] A. Azizzadeh, R. Mohammadkhani and S. V. A. Makki, "BER performance of uplink massive MIMO with low-resolution ADCs," 2017 7th International Conference on Computer and Knowledge Engineering (ICCKE), Mashhad, 2017, pp. 298-302.
- [9] IEEE 802.15.4-2015 - IEEE Standard for Low-Rate Wireless Networks. [https://standards.ieee.org/standard/802\\_15\\_4-2015.html](https://standards.ieee.org/standard/802_15_4-2015.html)
- [10] Isnain Arif Wicaksono, Soo Young Shin, Performance Evaluation of MIMO Spatial Multiplexing scheme on IEEE 802.15.4.
- [11] M. Elkourdi, A. Mazin and R. D. Gitlin, "Slotted Aloha-NOMA with MIMO Beamforming for Massive M2M Communication in IoT Networks," 2018 IEEE 88th Vehicular Technology Conference (VTC-Fall), Chicago, IL, USA, 2018, pp. 1-5.
- [12] Sanjib Sur, Teng Wei, and Xinyu Zhang. 2015. Bringing Multi-antenna Gain to Energy-constrained Wireless Devices. In ACM IPSN.
- [13] I. Sohn and D. Gwak, "Single-RF MIMO-OFDM system with beam switching antenna," EURASIP J. Wireless Commun. Netw., vol. 2016, no. 1, pp. 1-14, Dec. 2016.
- [14] A. Mohammadi and F. M. Ghannouchi, "Single RF front-end MIMO transceivers," IEEE Commun. Mag., vol. 49, no. 12, pp. 104-109, Dec. 2011